DNA Nanotechnology Hot Paper

International Edition: DOI: 10.1002/anie.201601042
German Edition: DOI: 10.1002/ange.201601042

Daisy Chain Rotaxanes Made from Interlocked DNA Nanostructures

*Johannes Weigandt[+], Chia-Ling Chung[+], Stefan-S. Jester, and Michael Famulok**

Abstract: *We report the stepwise assembly of supramolecular daisy chain rotaxanes (DCR) made of double-stranded DNA: Small dsDNA macrocycles bearing an axle assemble into a pseudo-DCR precursor that was connected to rigid DNA stoppers to form DCR with the macrocycles hybridized to the axles. In presence of release oligodeoxynucleotides (rODNs), the macrocycles are released from their respective hybridization sites on the axles, leading to stable mechanically interlocked DCRs. Besides the expected threaded DCRs, certain amounts of externally hybridized structures were observed, which dissociate into dumbbell structures in presence of rODNs. We show that the genuine DCRs have significantly higher degrees of freedom in their movement along the thread axle than the hybridized DCR precursors. Interlocking of DNA in DCRs might serve as a versatile principle for constructing functional DNA nanostructures where the movement of the subunits is restricted within precisely confined tolerance ranges.*

The development of dynamic DNA nanotechnology has led to functional molecular architectures and circuits with properties that can be operated in response to external stimuli.[1] Examples include DNA nanomachines[2] that can be switched, often reversibly, from one state to another,[3] motor systems based on DNA walkers,[4] DNA spiders,[5] polymerization,[6] and other systems.[7] The ultimate aim is to assemble autonomously working modules of DNA into multicomponent nanostructures in which different functions are combined to perform tasks of increasing complexity. However, assembling many different individual precursors into complex supramolecules that exhibit functions similar to large biological nanomachines still remains challenging. Therefore, concepts and tools for shaping, holding, positioning, programming, guiding, and assembling functional molecular architectures from a broad variety of different precursors are needed.[8]

[*] Dipl.-Chem. J. Weigandt,[+] Dr. C.-L. Chung,[+] Prof. Dr. M. Famulok
LIMES Chemical Biology Unit, Universität Bonn
Gerhard-Domagk-Strasse 1, 53121 Bonn (Germany)
E-mail: m.famulok@uni-bonn.de
Dr. S.-S. Jester
Kekulé-Institut für Organische Chemie und Biochemie
Universität Bonn
Gerhard-Domagk-Strasse 1, 53121 Bonn (Germany)
Prof. Dr. M. Famulok
Center of Advanced European Studies and Research
Ludwig-Erhard-Allee 2, 53175 Bonn (Germany)
[+] These authors contributed equally to this work.
Supporting information and the ORCID identification number(s) for the author(s) of this article can be found under http://dx.doi.org/10.1002/anie.201601042.

In analogy to macroscopic engineering, it will be advantageous for the DNA nanoengineering field to achieve control of directed movement within defined margins as opposed to diffusion-determined motion. In many biological machines, precisely guided bearing of moving components is essential to achieve proper function.[1b] Guide bearings in complex biological machines include the kinesin shuttle, sarcomeres, F_1-ATPase, or the bacterial flagellum.[9] Molecular guide bearings in biological machines ensure biomechanical movement to occur within precise margins, and similar concepts are required to construct complex DNA-based biohybrid machines. In DNA nanotechnology, however, solutions for this purpose are scarce.

Herein we report an approach based on interlocked daisy chain rotaxane (DCR) DNA nanostructures. In a DCR, a macrocycle connected to an axle bearing a stopper at its end circumscribes the axle of a second such unit and vice versa (Figure 1a; Figure 2a). Synthetic molecular DCRs are well-established.[10] In contrast, although interlocked DNA topologies such as catenanes,[11] borromean rings,[12] and rotaxanes[13] are known,[14] DNA nanostructures that form DCRs are unprecedented. To approach the concept of potential guide bearing by interlocked structures, we reasoned that DNA DCRs provide an ideal starting point to introduce movable components into nanorobotic structures that require operation within precise margins.

To construct a DCR architecture based on double-stranded DNA (dsDNA), we assembled two pairs of branched DNA macrocycles, 126R1/126R2 and 126X/126Y, respectively (Figure 1a; Scheme S1 and Figure S1 in the Supporting Information). Both macrocycle pairs consist of intrinsically bent AT tracts that entail unstrained circularization of dsDNA. From each macrocycle, a linear dsDNA sequence, rod-m1/rod-m2 for 126R1/126R2 and rodX/rodY for 126X/126Y, respectively, divert in a three-way junction. Rod-m1 contains an 8-mer ss-gap region that is complementary to 8 nt of the 12-mer gap in 126R2; rod-m2 was designed analogously with an 8-mer ss gap that hybridizes to 8 nt of the 12-mer gap in 126R1. RodX has a 9-mer ss region complementary to 9 nt of the 15-mer gap in 126Y and vice versa for the rodY/126X-pair (Figure 1a; Figure S1 and Table S1). When equimolar ratios of 126R1/126R2 or 126X/126Y are incubated at 15 °C, the two complementary ss gaps in the macrocycles and the axles hybridize with their respective counterpart to result in a pseudo-DCR with hybridized and thus immobile macrocycles.[15] In 126R1/126R2, each of the rods terminates with identical 5 nt overhangs; in 126X/126Y they terminate with two different sticky ends. The sticky ends can be used for attaching stopper molecules that prevent the interlocked DCR from dethreading once the hybridization between axles and macrocycle are released by means of the 12-mer release oligodeoxynucleotides (rODNs) L1/L2 for

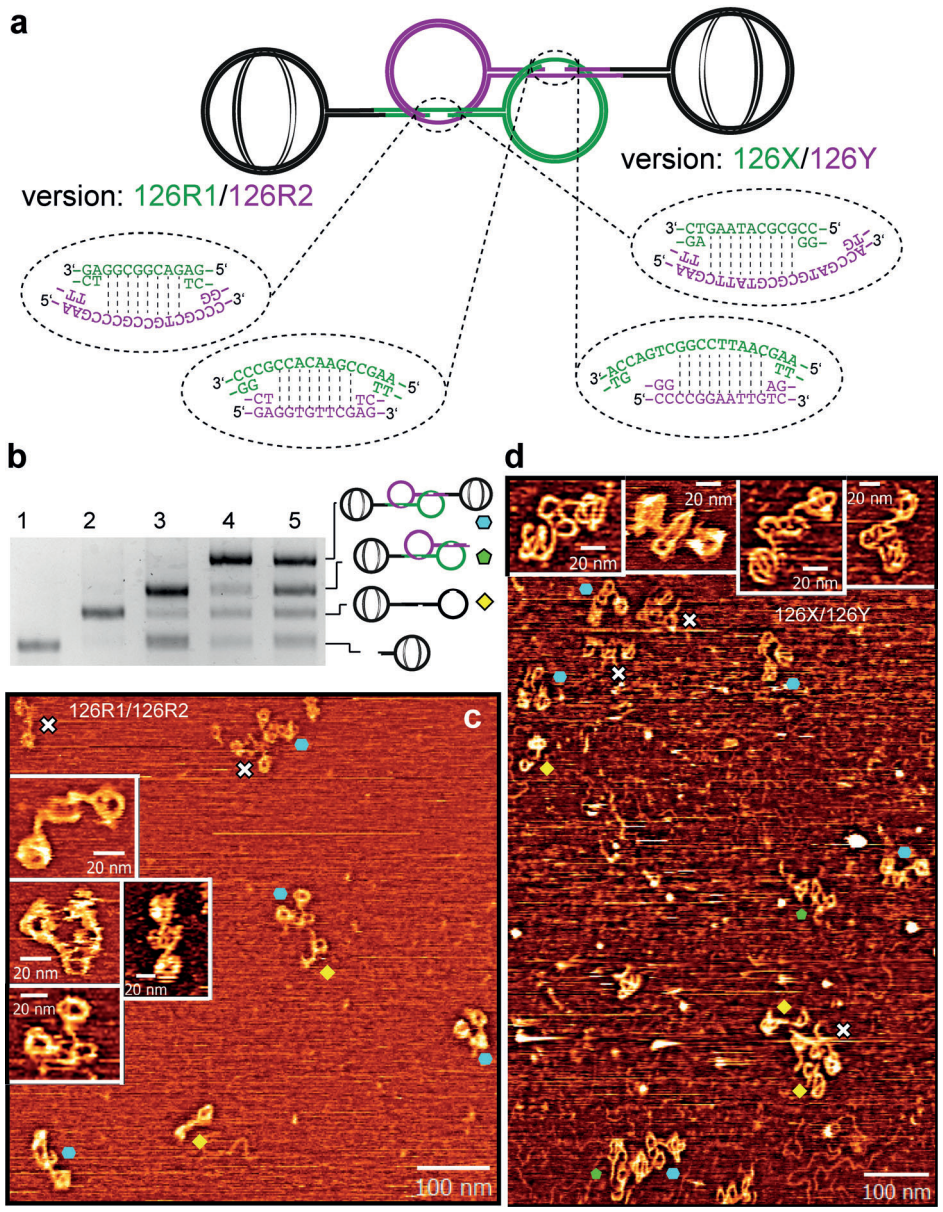

Figure 1. A stable, hybridized dsDNA daisy chain rotaxane (DCR^{hyb}).[15] a) Two different designs of DCR^{hyb} in which the macrocycles are hybridized to the axles (dotted lines encircling both gap regions). b) Electrophoretic mobility measured by agarose gel electrophoresis of DCR^{hyb} bearing spherical stoppers. Lanes 1–3: separately assembled individual substructures; lane 4: DCR^{hyb} 126R1/126R2; lane 5: DCR^{hyb} 126X/126Y. Blue, green, and yellow dots indicate the DCR^{hyb}, DCR^{hyb} minus one stopper, and dumbbell structures. c) High-resolution intermittent contact mode AFM scans of structures isolated from the main band in lane 4 (containing the DCR^{hyb} 126R1/126R2) at the mica/poly-L-ornithine/H_2O interface. White crosses indicate ambiguous structures. d) The same measurements for the structures isolated from the main band in lane 5 (containing the DCR^{hyb} 126X/126Y) at the mica/poly-L-ornithine/H_2O interface. Blue/green/yellow dots/white crosses in (c): 4:0:2:2; (d): 5:2:3:3. For an overview of the AFM images, see Figure S6a,b.

126R1/126R2, or XL/YL for 126X/126Y, respectively (Figure 1a; Figure S1 and Table S1). Using stoppers with different sticky ends slightly increases the amount of the single-stoppered pseudo-DCR (Figure 1b, lane 5) compared to the one in lane 4.

As stoppers, we ligated branched DNA crossover macrocycles composed of 168 base pairs[13b] (Figure S1; Table S1) to the sticky ends of each axle. The stopper size was chosen so as to preclude dethreading of the macrocycles, as established in previous studies.[13a,b] Figure 1b shows the electrophoretic mobility of individual fragments of the assembly; the resulting raw product of DCR^{hyb} forms as the main product. The architectures of DCR^{hyb} 126R1/126R2 (Figure 1c, Figure S5-1) and DCR^{hyb} 126X/126Y (Figure 1d, Figure S5-2) were confirmed by atomic force microscopy (AFM) in high-resolution intermittent contact mode at the mica/H_2O interface to form variably bent structures after adsorption to poly-L-ornithine as adhesive. However, in addition to four intact DCR^{hyb} species of 126R1/126R2 (Figure 1c, blue dots), two dumbbells (yellow dots), and two unspecified structures (crosses) were observed. For 126X/126Y we found five DCR^{hyb} (Figure 1d, blue dots), two DCR^{hyb} minus one stopper unit (green dots), three dumbbells (yellow dots), and three unspecified structures (crosses). The mechanism leading to the formation of the incomplete structures is unclear at this stage; however, the loss of a stopper from otherwise intact DCR^{hyb} justifies the assumption of a mechanical bond rupture, likely during adsorption, since dehybridization can be excluded because of ligation.

We added and ligated the rODNs L1/L2 for 126R1/126R2, or XL/YL for 126X/126Y to purified DCR^{hyb}. The rODNs are all fully complementary to the 12- or 15-mer ss gaps in the respective macrocycles (Figure 2a, step 1). Likewise, we added and ligated the rODNs S1/S2 for 126R1/126R2, or XS/YS for 126X/126Y, respectively, that are complementary to the ss gaps in the respective axles (Figure 2a, step 2). In the presence of the rODNs, both DCR^{hyb} structures convert into a product with slightly increased electrophoretic mobility, despite the increase in molecular weight (Figure 2b, upper panel; compare lane 2 with lane 4 for 126R1/126R2, and lane 3 with lane 5 for 126X/126Y). The differences in electrophoretic mobility were quantified by measuring the intensity profiles of the upper bands in each lane (Figure 2b, lower panel). The maxima of

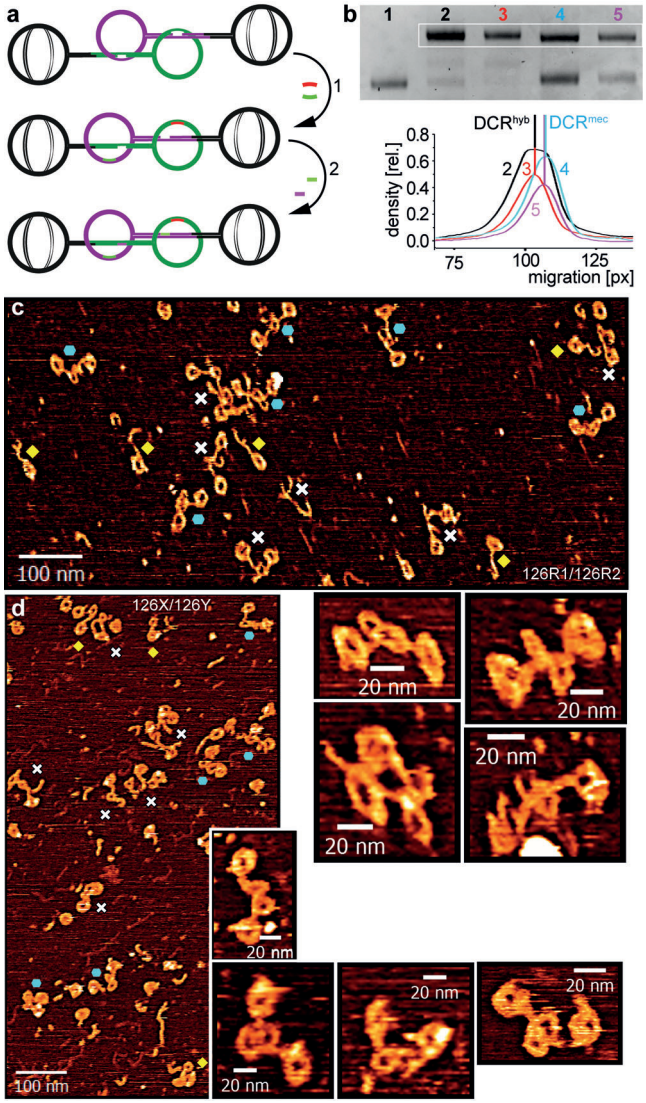

Figure 2. A stable double-stranded DNA daisy chain rotaxane. a) Formation of interlocked DNA daisy chain rotaxane (DCR^{mec}) from hybridized DCR^{hyb}. Step 1: addition and ligation of release ODNs L1, L2 (12-mers for 126R1/126R2), or XL, YL (15-mers for 126X/126Y) complementary to the ring-gap sequences. Step 2: addition and ligation of two shorter ODNs S1, S2 (8-mers for 126R1/126R2), or XS, YS (9-mers for 126X/126Y) complementary to the tail-gap sequences. b) Electrophoretic mobility of DCR^{mec} structures measured by agarose gel electrophoresis (upper panel). Lane 1: seperately assembled dumbbell with one 126R1 ring ligated to one spherical stopper; lanes 2, 3: reference samples (purified by agarose gel electrophoresis) of DCR^{hyb} (lane 2: 126R1/126R2; lane 3: 126X/126Y); lanes 4, 5: interlocked DCR^{mec} form after addition and ligation of all necessary release ODNs (lane 4: 126R1/126R2, lane 5: 126X/126Y). Lower panel: Intensity profiles of lanes (see white frame) confirm reduced electrophoretic mobility for the DCR^{hyb} (2, 3) versus DCR^{mec} structure (4, 5). c) High-resolution intermittent contact mode AFM images at the solid/liquid interface of the DCR^{mec} structures in lane 4 (126R1/126R2). d) The same measurement for the DCR^{mec} structures in lane 5 (126X/126Y).

the density profiles belonging to the DCR indicate that both DCR^{mec} versions (lanes 4 and 5) migrate slightly faster than the corresponding DCR^{hyb} structures (lanes 2 and 3), a phenomenon we have observed for other interlocked DNA nanostructures.[13a–c,16] Interestingly, the lower bands in lanes 4 and 5, which correspond to the dumbbells that form after addition of the rODNs, differ significantly in their intensities (Figure 2b, upper panel), thus indicating that ring and axle gaps hybridize to some extent externally, that is, without interlocking. In the 126X/126Y pair, this external hybridization occurs less frequently than in the 126R1/126R2-system, which likely arises from the additional base pair in the former system.

The structures shown in lanes 4 and 5, respectively, were deposited onto mica using the adhesive poly-L-ornithine. Figure 2c,d shows the high-resolution AFM images acquired at the solid/liquid interface of mechanically interlocked 126R1/126R2 and 126X/126Y DCR^{mec} species (for additional overview images, see Figure S7a,b).[15] For native DCR^{mec}, the spherical stoppers and the interlocked DCR motifs are both clearly resolved. However, several dumbbell structures are found (Figure 2c,d; yellow dots), consistent with the additional bands observed in the lower parts of the gels after electrophoretic separation (Figure 2b, lanes 4, 5). In addition, nonspecified fragments (e.g. rings, ring/axle structures, and short linear segments) are observed (Figure 2c,d; crosses).

However, we noted during DCR^{mec} assembly that a small amount of dumbbell monomers form after addition of rODNs, despite DCR^{mec} being mechanically stable. The most likely reason for this observation is a certain level of imperfect interlocking, where only one or no ring/axle pair is interlocked while the other one hybridizes externally (Figure 3a, upper left structure). In the presence of rODNs, the interlocked part of the structure dehybridizes, and the formerly interlocked macrocycle dethreads in a slippage mechanism, as previously observed for dsDNA rotaxanes,[13e] to result in the dumbbell-monomers (Figure 3a). Because purification of DCR^{hyb} occurred in the presence of buffer throughout the entire process, the externally hybridized structures can potentially survive purification.

To test this hypothesis and to determine the proportion of external hybridization of two noninterlocked dumbbells versus the interlocked DCR^{mec}, the level of hybridized dumbbell dimers that form when the noninterlocked 126R1 and 126R2 dumbbells hybridize externally was analyzed by nondenaturing agarose gel electrophoresis. As references, a single 126R1 dumbbell, and the purified DCR^{hyb} 126R1/126R2 were used. We observed around 30% of a band corresponding to the dimerized form of externally hybridized dumbbells, whereas around 70% of the dumbbells remained as monomers (Figure 3b). Thus, a significant proportion of noninterlocked 126R1/126R2 hybridize at the ring exterior, and a semi-interlocked DCR^{hyb} structure should be even more stable. Therefore, the purification of DCR^{mec} must be performed in presence of rODNs to avoid unintended copurification of semi- or noninterlocked dimers. This strategy becomes more important when assembling DCR^{mec} in which incompletely interlocked components do not fall apart into smaller fragments after rODN addition, but remain at the same size as the desired structure, thus being incompatible with gel purification.

We next analyzed the effect of consecutive addition of rODNs on the transformation of DCR^{hyb} into DCR^{mec}. We

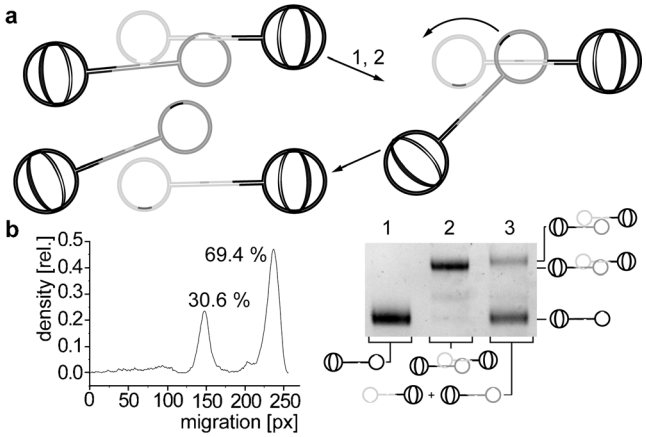

Figure 3. Different threading states lead to partial interlocking. a) Example of one possible form generated during the assembly of DCR^{hyb}: a pseudo-DCR,[15] where the tail gap of 126R1 hybridizes externally, i.e., without interlocking to the ring gap in 126R2. Steps 1 and 2: successive addition of the corresponding rODNs to release the hybridized gaps leads to a semi-interlocked pseudo-DCR, which dethreads in a slippage process, giving rise to the dumbbells. b) Right panel: Mobility of both noninterlocked dumbbells to quantify the extent of external hybridization. Lane 1: dumbbell reference; lane 2: DCR^{hyb}; lane 3: combination of dumbbell 126R1 and dumbbell 126R2 with all ss gaps available for hybridization. The appearance of the upper band indicates formation of a DNA structure in which the dumbbells hybridize without interlocking. Left panel: Intensity profile of the same agarose gel showing the level of external hybridization.

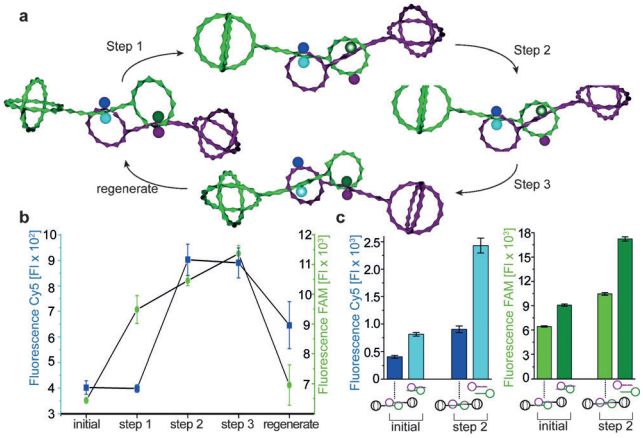

Figure 4. Dual-labeled DCR with fluorophore–quencher pairs Cy5/BHQ3 and FAM/BHQ1. a) Switching between distinct states. Switching conditions: see the Supporting Information. b) Switching steps versus fluorescence intensities of Cy5 (cyan *y*-axis) and FAM (green *y*-axis). c) Comparison of fluorescence intensities of DNA DCR^{hyb} with 126R1/126R2 (see Figure S4), focusing on the initial state and step 2.

sought to find evidence for structures where DCR^{hyb} and DCR^{mec} exist in the same molecule, that is, $DCR^{hyb/mec}$, and only one of the rings becomes released while the other remains hybridized. DCR were labeled with fluorophore/quencher pairs at the hybridization sites (Figure 4a). 126R1 contained Cy5 at the tail gap (cyan sphere) and black-hole quencher 1 (BHQ1) at the ring gap (purple sphere); 126R2 contained FAM at the tail gap (green sphere) and BHQ3 at the ring gap (blue sphere). Toehold (TH) versions of the rODNs (TH1, TH2) released the rings from their hybridization with the axles. To restore DCR^{hyb} by removing TH1 and/or TH2, we used *anti*-TH-ODNs (AH1, AH2) complementary to the TH-rODNs (Figure S2). A series of control experiments were performed to compare the data measured with the DCR^{hyb} and DCR^{mec} systems. Firstly, we determined the level of external hybridization by fluorescence quenching (FQ) of a FAM- and a BHQ1-labeled dumbbell pair (Figure S3, upper left panel). External hybridization minimized the quenching of the FAM fluorescence after mixing the labeled dumbbells (Figure S3, lower left panel). Secondly, we tested the efficiency of rODN-hybridization by adding a BHQ1-labeled TH1 to the FAM-labeled 126R1 dumbbell and found that hybridization occurred with high efficiency (Figure S3, right panel). Thirdly, we omitted the stoppers in the DCR-structure and performed the same set of experiments with this pseudo-DCR. The lack of stable interlocking means that the presence of any rODN leads to more rapid disassembly of pseudo-DCR than of DCR^{hyb} or DCR^{mec}, and to higher absolute levels of fluorescence dequenching (Figure 4c; Figure S4). Starting from DCR^{hyb} (Figure 4a, left-hand side; and Figure 4b, initial) TH1 addition led to a fluorescence increase of FAM, but not Cy5 (Figure 4b, step 1). Addition of TH2 further increased the FAM fluorescence, and maximized that of Cy5, thus indicating the formation of DCR^{mec} (step 2). No significant change in the fluorescence levels of both fluorophores was observed with AH1 (step 3), whereas regeneration of FAM quenching and partial regeneration of Cy5 quenching resulted from addition of AH2 (Figure 4b, regenerate). The nonstoppered structure always had higher absolute fluorescence levels than DCR^{mec} or DCR^{hyb}.

Finally, we measured the distances between the edges of the macrocycle and the spherical stoppers in individual DCR^{hyb} and DCR^{mec} structures by using AFM (Figure S5). Both structures deviate from idealized DCRs because of the flexibility of dsDNA. Notwithstanding, the stopper/macrocycle distances for 15–25 individual DCR^{hyb} and DCR^{mec} structures were, within experimental error, identical in DCR^{hyb} on both sides of the structure (126R1/126R2: 14 ± 1 nm; 126X/126Y: 15 ± 1 nm), and the distribution was significantly smaller than in DCR^{mec}. In DCR^{mec}, we observed long and short median distances in each structure (126R1/126R2: 15 ± 5, 9 ± 3 nm; 126X/126Y: 15 ± 4, 9 ± 3 nm). Thus, L_{short} and L_{long} statistically deviate significantly more from the means in DCR^{mec} than in DCR^{hyb} (Figure S5). Together with the FQ analyses, these results provide clear evidence of higher mechanical freedom in DCR^{mec} along the axle margins than in DCR^{hyb}, where macrocycle mobility is highly confined.

To conclude, our study introduces an unprecedented class of interlocked dsDNA nanostructures, namely the daisy-chain rotaxane. We show that when assembling this architecture, about 30% of the structures incompletely interlock by external hybridization, thus leading to dethreading after release of the macrocycles from their hybridization sites in the axles by means of rODNs. This behavior must be taken into account when assembling more complex functional DNA

DCR structures. The DCRs represent interlocked DNA nanostructures in which the threaded stopper/axle/macrocycle units can move along a flexible dsDNA axle, thereby providing a functional mechanical element with the potential to serve as a slide bearing. Future dsDNA DCR systems with more rigid PX100 axles[13b] instead of a dsDNA axle might provide slide bearings consisting of several such interlocked units. More generally, mechanical daisy chain interlocking of DNA architectures might allow guided bearing in future dynamic DNA nanostructures in which the movement of parts requires guidance within a certain tolerance range to achieve defined levels of elasticity and to reduce friction between moving parts.

Acknowledgements

We thank D. Ackermann, J. Valero, and M. Monteverde for helpful discussions, and the ERC (grant 267173) for support.

Keywords: daisy chain rotaxanes · DNA structures · DNA nanotechnology · nanostructures · supramolecular chemistry

[1] a) U. Feldkamp, C. M. Niemeyer, *Angew. Chem. Int. Ed.* **2006**, *45*, 1856; *Angew. Chem.* **2006**, *118*, 1888; b) M. G. van den Heuvel, C. Dekker, *Science* **2007**, *317*, 333; c) D. Y. Zhang, G. Seelig, *Nat. Chem.* **2011**, *3*, 103; d) Y. Krishnan, F. C. Simmel, *Angew. Chem. Int. Ed.* **2011**, *50*, 3124; *Angew. Chem.* **2011**, *123*, 3180.

[2] J. Bath, A. J. Turberfield, *Nat. Nanotechnol.* **2007**, *2*, 275.

[3] a) Y. Kamiya, H. Asanuma, *Acc. Chem. Res.* **2014**, *47*, 1663; b) H. Nishioka, X. Liang, T. Kato, H. Asanuma, *Angew. Chem. Int. Ed.* **2012**, *51*, 1165; *Angew. Chem.* **2012**, *124*, 1191; c) V. Linko, H. Dietz, *Curr. Opin. Biotechnol.* **2013**, *24*, 555; d) T. Gerling, K. F. Wagenbauer, A. M. Neuner, H. Dietz, *Science* **2015**, *347*, 1446.

[4] a) H. Gu, J. Chao, S. J. Xiao, N. C. Seeman, *Nature* **2010**, *465*, 202; b) T. Omabegho, R. Sha, N. C. Seeman, *Science* **2009**, *324*, 67; c) W. B. Sherman, N. C. Seeman, *Nano Lett.* **2004**, *4*, 1203; d) P. Yin, H. Yan, X. G. Daniell, A. J. Turberfield, J. H. Reif, *Angew. Chem. Int. Ed.* **2004**, *43*, 4906; *Angew. Chem.* **2004**, *116*, 5014.

[5] K. Lund, A. J. Manzo, N. Dabby, N. Michelotti, A. Johnson-Buck, J. Nangreave, S. Taylor, R. Pei, M. N. Stojanovic, N. G. Walter, E. Winfree, H. Yan, *Nature* **2010**, *465*, 206.

[6] S. Venkataraman, R. M. Dirks, P. W. Rothemund, E. Winfree, N. A. Pierce, *Nat. Nanotechnol.* **2007**, *2*, 490.

[7] a) M. K. Beissenhirtz, I. Willner, *Org. Biomol. Chem.* **2006**, *4*, 3392; b) M. Langecker, V. Arnaut, T. G. Martin, J. List, S. Renner, M. Mayer, H. Dietz, F. C. Simmel, *Science* **2012**, *338*, 932; c) E. R. Kay, D. A. Leigh, *Angew. Chem. Int. Ed.* **2015**, *54*, 10080; *Angew. Chem.* **2015**, *127*, 10218.

[8] J. J. Funke, H. Dietz, *Nat. Nanotechnol.* **2016**, *11*, 47.

[9] Y. Hizukuri, S. Kojima, M. Homma, *J. Biochem.* **2010**, *148*, 309.

[10] a) O. Lukin, F. Vögtle, *Angew. Chem. Int. Ed.* **2005**, *44*, 1456; *Angew. Chem.* **2005**, *117*, 1480; b) J. Rotzler, M. Mayor, *Chem. Soc. Rev.* **2013**, *42*, 44; c) J. F. Stoddart, *Chem. Soc. Rev.* **2009**, *38*, 1802.

[11] a) J. Elbaz, A. Cecconello, Z. Fan, A. O. Govorov, I. Willner, *Nat. Commun.* **2013**, *4*, 2000; b) J. Elbaz, Z. G. Wang, F. Wang, I. Willner, *Angew. Chem. Int. Ed.* **2012**, *51*, 2349; *Angew. Chem.* **2012**, *124*, 2399; c) D. Han, S. Pal, Y. Liu, H. Yan, *Nat. Nanotechnol.* **2010**, *5*, 712; d) T. Li, M. Famulok, *J. Am. Chem. Soc.* **2013**, *135*, 1593; e) Y. Sannohe, H. Sugiyama, *Bioorg. Med. Chem.* **2012**, *20*, 2030; f) T. L. Schmidt, A. Heckel, *Nano Lett.* **2011**, *11*, 1739; g) T. Li, F. Lohmann, M. Famulok, *Nat. Commun.* **2014**, *5*, 4940.

[12] C. D. Mao, W. Q. Sun, N. C. Seeman, *Nature* **1997**, *386*, 137.

[13] a) D. Ackermann, T. L. Schmidt, J. S. Hannam, C. S. Purohit, A. Heckel, M. Famulok, *Nat. Nanotechnol.* **2010**, *5*, 436; b) D. Ackermann, S.-S. Jester, M. Famulok, *Angew. Chem. Int. Ed.* **2012**, *51*, 6771; *Angew. Chem.* **2012**, *124*, 6875; c) F. Lohmann, D. Ackermann, M. Famulok, *J. Am. Chem. Soc.* **2012**, *134*, 11884; d) S. Bi, Y. Cui, L. Li, *Analyst* **2013**, *138*, 197; e) F. Lohmann, J. Weigandt, J. Valero, M. Famulok, *Angew. Chem. Int. Ed.* **2014**, *53*, 10372; *Angew. Chem.* **2014**, *126*, 10540.

[14] S.-S. Jester, M. Famulok, *Acc. Chem. Res.* **2014**, *47*, 1700.

[15] We suggest the terms DCR^{hyb} and DCR^{mec} to discriminate the immobile (hybridized) from the mobile (mechanically interlocked) macrocycles in the daisy chain rotaxanes. The DCR structures that lack one or both stopper units are called pseudo-DCR. Pseudo-DCR are only stable in the hybridized form (pseudo-DCR^{hyb}) and disassemble into the dumbbell structures in the presence of release oligodeoxynucleotides (rODNs). These terms refer best to IUPAC nomenclature for rotaxanes; see: J. Vohlídal, E. S. Wilks, A. Yerin, A. Fradet, K. H. Hellwich, P. Hodge, J. Kahovec, W. Mormann, R. F. T. Stepto, *Pure Appl. Chem.* **2012**, *84*, 2135.

[16] F. Lohmann, J. Valero, M. Famulok, *Chem. Commun.* **2014**, *50*, 6091.

Received: February 4, 2016
Revised: March 3, 2016
Published online: ■■ ■■, ■■■■

Communications

DNA Nanotechnology

J. Weigandt, C.-L. Chung, S.-S. Jester, M. Famulok* ——— ■■■■–■■■■

Daisy Chain Rotaxanes Made from Interlocked DNA Nanostructures

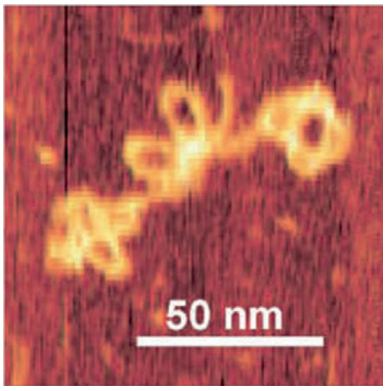

Chained up: Mechanically bonded daisy chain rotaxanes (DCRs) made from double-stranded DNA (dsDNA) comprise a macrocycle connected to an axle bearing a stopper at its end that circumscribes the axle of a second such unit and vice versa (see image). Mechanically interlocked DCRs have higher degrees of freedom in their movement along the thread axle than the DCR-precursors in which the macrocycles are still hybridized to the axle.